

Supporting Information for

**Low-Temperature Study of Hydrogen-Bond Symmetry in Cyclohexene-1,2-dicarboxylate
Monoanion in an Organic Medium**

Charles L. Perrin* and Kathryn D. Burke

Department of Chemistry, University of California—San Diego

La Jolla, CA 92093-0358 USA

cperrin@ucsd.edu

Experimental

Materials. 4,5,6,7-Tetrahydro-1,3-isobenzofurandione (cyclohexene-1,2-dicarboxylic anhydride, 3,4,5,6-tetrahydrophthalic anhydride, Aldrich) was recrystallized from diethyl ether (mp 69–75°C, lit¹ 70.6–72°C). Tetrabutylammonium hydroxide (Aldrich, 40 wt % in water) was standardized by titration with 1.000 ± 0.005 M HCl. H₂¹⁸O in 1 mL ampoules (Cambridge Isotope Labs, 97% ¹⁸O) was used without additional purification. THF (Aldrich, >99.9% anhydrous) and CDCl₃ (Cambridge Isotope Labs) were used without additional purification.

NMR Methods. The ¹H NMR spectra were collected with a window of 13.8 kHz (0 ppm to 22 ppm) to include any deshielded OHO signal. Reasonable ¹H spectra were obtained with four transients and 16K points.

The 125-MHz ¹³C NMR spectra were obtained using a heteronuclear broad band probe with ¹H decoupling centered at 2 ppm. The probe was tuned to the sample prior to gradient shimming. A spectral window of 8000 Hz (125 ppm to 185 ppm) was used with 32k data points and zero-filled to a final resolution of 64 points/Hz. Spectra were collected with between 64 and 256 transients. Line broadening of 0–1.0 Hz was applied, depending on the resolution and the presence of fine splitting. ¹H and ¹³C NMR acquisitions were obtained at a temperature range from 20°C to –60°C. For each temperature, the probe was set to the desired temperature and allowed to equilibrate for 10 minutes before spectra were obtained. The probe was tuned and the sample was shimmed at each temperature. Spectra were processed using JEOL Delta 5.0.2 and

ACD/NMR Processor Academic Edition.

The temperature in the NMR probe was calibrated using 4% methanol in methanol- d_4 .² Temperatures were allowed to equilibrate for 12 minutes before the spectrum was acquired. The difference between the set T and the actual T was generally less than 1°C at any given temperature, and the actual temperatures were used for all the analyses herein.

Synthesis of 5- $^{18}\text{O}_{0-4}$. A mixture of ^{18}O isotopologues of cyclohexene-1,2-dicarboxylic acid **6** was synthesized by combining 20 mg (0.1 mmol) of the anhydride with 20.0 μL H_2^{18}O and 50–70 μL anhydrous THF (to increase solubility) in a 3 mL conical reaction vessel equipped with a spin vane. The reaction mixture was stirred at room temperature for 20–24 hours. The extent of hydrolysis was monitored by thin layer chromatography on activated silica (eluted with 100% EtOAc; anhydride reactant R_f : 0.63; diacid **6** product R_f : 0.20). Increasing incorporation of ^{18}O with time was confirmed by mass spectrometry of **6**. Reversion of **6** to the anhydride during degassing interferes with thorough characterization by NMR. The solid tetrabutylammonium salt of the monoacid monoanion **5** was then obtained by adding 1 equivalent (based on anhydride) of tetrabutylammonium hydroxide to the reaction vessel containing **6** and removing the solvent via vacuum pump. No purification was performed. ^1H NMR (CDCl_3): 0.91 ppm (t, H_δ , 14H), 1.33 ppm (m, H_γ , 9H), 1.48 ppm (m, H_α , 4H), 1.54 ppm (m, H_β , 9H), 2.44 ppm (m, H_b , 4H), 3.17 ppm (m, H_α , 9H), 19.9 ppm (bs, OH). ^{13}C NMR (CDCl_3): 13.6 ppm, 19.7 ppm, 22.3 ppm, 23.9 ppm, 29.4 ppm, 58.7 ppm, 139.3 ppm, 171.3 ppm.

Negative-ion mass spectrometry of ^{18}O -labeled diacid **6** ($[\text{M}-\text{H}]^- = 169$ m/z for $\text{C}_8\text{H}_9\text{O}_4^-$) was used to measure $P(n)$ ($n = 0,1,2,3,4$), the fraction of the resulting ion **5** that is un-, mono-, di-, tri-, or tetra-labeled. The values are presented in Table 1, corrected for ^{13}C content. Although each preparation produced slightly different ratios, they were all very similar, and this table is representative of all samples.

NMR Sample Preparation and NMR Spectra. NMR samples were prepared as 0.1 M **5- $^{18}\text{O}_{0-4}$** in CDCl_3 . Samples were deoxygenated using the freeze-pump-thaw method and used without further drying. At each temperature a ^1H NMR spectrum was acquired before acquiring

^{13}C NMR data.

The presence of **5** was confirmed by ^1H NMR. Figure S1 shows the ^1H NMR spectrum for a mixture of ^{18}O -labeled isotopologues of **5** at 233 K. The signals representing H_a and H_b of the cyclohexene ring appear about 0.94 ppm apart from each other. This is indicative of monoanion **5**, because the diacid **6**, the dianion (in water), and the anhydride starting material all have smaller peak separations. The acidic proton is highly deshielded and appears at about 20 ppm. At room temperature this signal is very broad and disappears into the baseline. At lower temperatures this signal begins to be visible, as shown in Figure S1, although it is still too broad for an accurate integration.

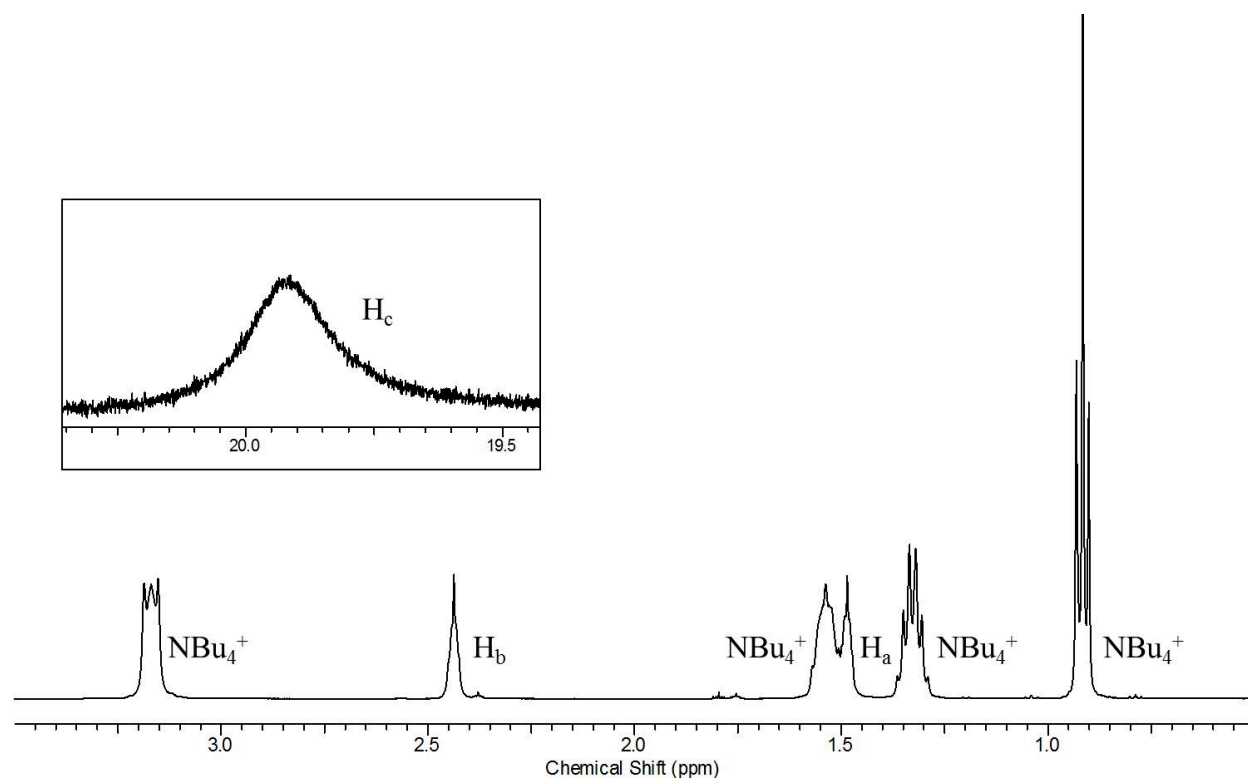


Figure S1. ^1H NMR spectrum of a mixture of ^{18}O -labeled isotopologues of **5** in CDCl_3 at 233 K, where the acid proton at 20 ppm is visible.

According to the integration of H_b at 2.44 ppm against H_α of Bu_4N^+ at 3.35 ppm, there is a 17% excess of tetrabutylammonium counterion in the sample. This implies that some other anion

is present. A silver test ruled out the presence of halides. This impurity is likely to be the dianion, owing to weighing errors at milligram quantities. If the exchange between the monoanion and the dianion were slow there would be additional signals from the dianion, but these are not seen. Therefore, the exchange between the monoanion and dianion must be rapid so that the observed H_a and H_b signals are 83:17 averages of monoanion and dianion. Yet even if the impurity is the dianion, its presence would only reduce an observed perturbation of the equilibrium, so that this complication can be ignored for the conclusions herein.

Chemical-Shift Assignments for Carboxyl Carbons in ^{18}O Isotologues of monoanion 5. Figure 1 shows the ^{13}C NMR signals for the carboxyl carbons. Signals are assigned as unlabeled (\mathbf{A}_0), mono- ^{18}O -labeled (\mathbf{A}_1), and di- ^{18}O -labeled (\mathbf{A}_2). Table S1 lists their relative intensities (peak heights).

Table S1. Relative peak heights h of each ^{18}O -labeled carboxyl carbon in Figure 1 and the distribution $p(r)$ ($r = 0,1,2$) derived from mass intensities in Table 1.

Signal	h	$p(r)$
\mathbf{A}_0	0.403	0.381
\mathbf{A}_1	0.461	0.472
\mathbf{A}_2	0.136	0.146

Those intensities can be compared with intensities estimated independently from the mass-spectrometric $P(n)$ in Table 1. The average number of ^{18}O labels per molecule, $\langle^{18}\text{O}\rangle$, is 1.530, the weighted sum $\sum nP(n)$ of those probabilities. This, divided by 4, the maximum ^{18}O content, gives the probability $p(^{18}\text{O}) = 0.382$ that any oxygen is ^{18}O . The probability $p(r)$ ($r = 0,1,2$) that 0, 1, or 2 ^{18}O labels are bonded to a carboxyl carbon is then given by the binomial distribution, as expressed in Equation S1. These probabilities are included in Table S1. They match very well the relative peak heights from Figure 1, with a root-mean-square deviation of only 0.015. This agreement supports the \mathbf{A}_0 , \mathbf{A}_1 , and \mathbf{A}_2 assignments.

$$p(r) = \frac{2!}{r!(2-r)!} p(^{18}\text{O})^r [1 - p(^{18}\text{O})]^{1-r} \quad (\text{S1})$$

At increased resolution and with no applied line broadening the three signals in Figure 1 separate into additional signals, as shown in Figure 2. The signals are designated so that the first subscript is the number of ^{18}O s attached to a carboxyl carbon, as in Figure 1, while the second subscript represents the number of ^{18}O s attached to the other carboxyl carbon. The justification for the signal assignments is as follows:

Figure 3 shows all six isotopologues of ^{18}O -labeled **5** with 0, 1, 2, 3, and 4 ^{18}O s, including two isotopomers, **5- $^{18}\text{O}_{2s}$** and **5- $^{18}\text{O}_{2a}$** , with two ^{18}O labels. Each of the isotopologues **5- $^{18}\text{O}_1$** , **5- $^{18}\text{O}_{2s}$** , and **5- $^{18}\text{O}_3$** , which have carboxyl groups with one ^{16}O and one ^{18}O , is present as a pair of conformational isotopomers, interconverted by rotation about the C–C bond. Because exchange between monoanion and dianion is rapid, as documented above, the rotation must also be rapid, via the dianion. The conformational isotopomers are analogous to $\text{RC}(=^{16}\text{O})\text{OH}$ and $\text{RC}(=\text{O})^{18}\text{OH}$, for which the tautomeric equilibrium constant has been estimated as 1.011,³ based on vibrational frequencies of carboxylic acids and carboxylate anions.⁴ Moreover, doubly ^{18}O -labeled monoanions show twice the isotope shift of the corresponding mono- ^{18}O -labeled monoanion.⁵ Therefore although only one conformational isotopomer is shown in Figure 3, both are present, and in equal amounts.

Within each structure there are both carboxyl carbons **A** and ipso carbons **B**, which are considered below. Three of these ions—**5- $^{18}\text{O}_0$** , **5- $^{18}\text{O}_{2s}$** , and **5- $^{18}\text{O}_4$** — are symmetrically substituted, with the same number of ^{18}O s attached to the two carboxyl groups. Their carboxyls are labeled as **A $_{00}$** , **A $_{11}$** , and **A $_{22}$** . The other three ions—**5- $^{18}\text{O}_1$** , **5- $^{18}\text{O}_{2a}$** , and **5- $^{18}\text{O}_3$** — where the two carboxyls have a different number of ^{18}O s, are asymmetrically substituted. Their carboxyls are labeled as **A $_{10}$** , **A $_{01}$** , **A $_{20}$** , **A $_{02}$** , **A $_{21}$** , and **A $_{12}$** .

The relative intensities (peak heights) h , as measured from Figure 2, are listed in Table S2. Also listed are the intensities calculated according to the following logic: We seek $p(r,r')$ ($r = 0,1,2$

= r'), the joint probability that a carboxyl bears $r = 0, 1,$ or 2 ^{18}O s while the other carboxyl bears $r' = 0, 1,$ or 2 ^{18}O s. Note that this must be distinguished from the per-molecule $P(n)$ ($n=0,1,2,3,4$) in Table 1. The probability of an unlabeled ion, $P(0)$, corresponds to $p(0,0)$, the intensity of the **A₀₀** signal, which arises from **5- ^{18}O ₀**, the only ion without an ^{18}O label. Similarly, the probability of a tetralabeled ion, $P(4)$, corresponds to $p(2,2)$, the (undetectable) intensity of the **A₂₂** signal. The other probabilities, $P(1)$, $P(2)$, and $P(3)$, are split among the remaining types of carboxyls. The probability of a monolabeled ion, $P(1)$, corresponds to the signals **A₀₁** and **A₁₀**. These carboxyls are on the same ion, and the intensity $P(1)$ must be split in half, with one half representing $p(0,1)$ and the other representing $p(1,0)$. Similarly, the probability of a trilabeled ion, $P(3)$, corresponds to a 50/50 mixture of **A₁₂** and **A₂₁**. The probability of a dilabeled ion, $P(2)$, corresponds to **A₁₁**, **A₀₂** and **A₂₀**. A second ^{18}O label is twice as likely to be on the distant carbon, resulting in **A₁₁**, than it is to be on an already labeled carbon, resulting in **A₀₂** and **A₂₀**. Thus $p(1,1)$ is equal to $2/3$ of the intensity $P(2)$ and $p(0,2)$ and $p(2,0)$ together are equal to $1/3$ of that intensity, or each is $1/6$ of that intensity. In this way each of the $p(r,r')$ in Table S2 can be derived. The values agree favorably with the measured peak heights h , with a root-mean-square deviation of 0.017. This agreement supports the assignments attached to Figure 2.

Table S2. Relative peak height h of each carboxyl carbon in Figure 2, assignments, and corresponding joint distribution $p(r,r')$ derived from per-molecule intensities $P(n)$ in Table 1.

Signal	5-^{18}O	Corresp	h	$p(r,r')$
A₀₂	2a	$1/6P(2)$	0.058	0.061
A₀₁	1	$1/2P(1)$	0.202	0.211
A₀₀	0	$P(0)$	0.135	0.089
A₁₂	3	$1/2P(3)$	0.054	0.058
A₁₁	2s	$2/3P(2)$	0.229	0.244
A₁₀	1	$1/2P(1)$	0.204	0.211
A₂₂	4	$P(4)$	— ^a	0.006

A₂₁	3	$^{1/2}P(3)$	0.055	0.058
A₂₀	2a	$^{1/6}P(2)$	0.063	0.061

^aNot visible because of low abundance.

Temperature Dependence of Carboxyl Shifts. As the temperature decreases, the chemical shifts of carboxyl carbons of ¹⁸O-labeled **5** move apart, as shown in Figure S2. At low temperatures the resolution deteriorates, so that the eight signals coalesce to three. This can be simulated (for sake of comparison) by applying a line broadening of 1 Hz to all spectra, which results in weighted averages across the unlabeled (**A₀**), mono-labeled (**A₁**) and di-labeled (**A₂**) carboxyl carbons. Their chemical shifts are listed in Table S3. Table S4 lists the temperature dependence of the chemical shift of each of the 8 carboxyl signals at temperatures where all are resolvable.

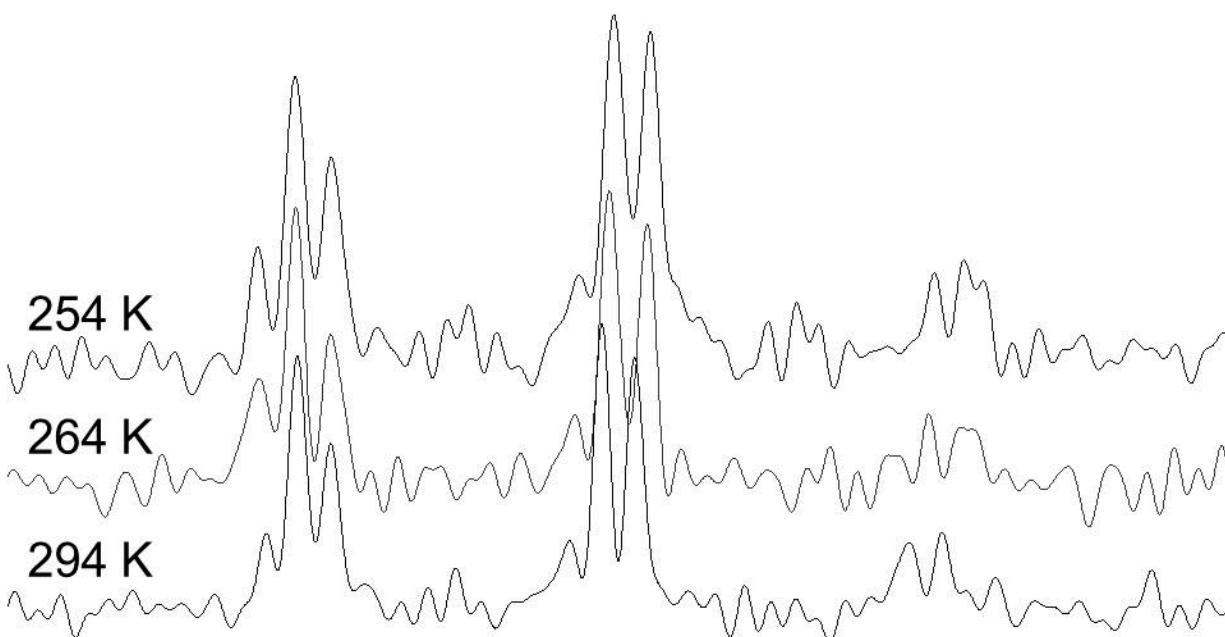


Figure S2. Temperature dependence of the ¹³C NMR signals of the carboxyl carbons in ¹⁸O isotopologues of **5**.

Table S3. ^{13}C chemical shifts (ppm) for carboxyl carbons of the ^{18}O isotopologues of **5** in CDCl_3 at various temperatures (K), with an applied line broadening of 1 Hz

Peak	293.9	264.1	254.1	244.2	224.3
A₀	171.3576	171.5139	171.5624	171.6205	171.7169
A₁	171.3266	171.4811	171.5294	171.5866	171.6829
A₂	171.2953	171.4481	171.4958	171.5538	171.6481

Table S4. ^{13}C chemical shifts (ppm) of the resolved carboxyl carbons in ^{18}O isotopologues of **5** in

CDCl_3 .			
Signal	293.9 K	264.1 K	254.1 K
A₀₂	171.3618	171.5185	171.5670
A₀₁	171.3587	171.5147	171.5628
A₀₀	171.3553	171.5110	171.5593
A₁₂	171.3312	171.4861	171.5347
A₁₁	171.3280	171.4826	171.5305
A₁₀	171.3247	171.4789	171.5269
A₂₁	171.2970	171.4503	171.4977
A₂₀	171.2937	171.4473	171.4945

Although $^1\Delta_0 + ^4\Delta_0$, from the separation between **A₁₁** and **A₀₀** of two symmetrically substituted ions, is an intrinsic isotope shift that ought to be independent of temperature, this value in Table 2 increases in magnitude by 1.5 ppb from 293.9 K to 254.1 K. Nevertheless, this increase is only apparent, arising from the poorer resolution at lower temperatures. As the resolution decreases, the signals begin to coalesce from eight signals to three, so that the signal containing **A₀₀** moves farther away from that containing **A₁₁**, as can be seen from their positions in Figure 2.

If the other three isotope shifts in Table 2 were solely intrinsic, they should remain nearly constant as the temperature decreases. The differences between the 293.9 K and 254.1 K values for

$-(^1\Delta - ^4\Delta)$ (or twice that) in Table 2 are 1.9 ppb, 2.7 ppb, and 4.4 ppb. Each of these is larger than the increase of 1.5 ppb observed for $-(^1\Delta_0 + ^4\Delta_0)$ in the first entry. The smaller increase was explained by coalescence of signals at low temperature. However, that argument does not hold for $^1\Delta - ^4\Delta$, because coalescence would move the signal containing **A₁₀** closer to that containing **A₀₁**, as can be seen from their positions in Figure 2, and likewise for the other two pairs. Therefore the coalescence would decrease each of the $^1\Delta - ^4\Delta$ differences, not increase them.

Chemical-Shift Assignments for Ipso Carbons in ¹⁸O Isotopologues of 5. The inability to resolve the chemical shifts of **B₁₁** and **B₀₀** within the signal labeled **B_{00/11}** leads to the conclusion that the intrinsic isotope shift $^2\Delta_0 + ^3\Delta_0$ is negligible. The alternative is that the two intrinsic isotope shifts $^2\Delta_0$ and $^3\Delta_0$ have opposite signs and nearly identical magnitudes, thus nearly canceling and resulting in no observable intrinsic isotope shift. However, it is highly unlikely that a two-bond shift and a three-bond shift have such similar magnitudes. Therefore a negligible intrinsic isotope shift is the more reasonable explanation.

The relative intensities (peak heights) h , as measured from Figure 4, are listed in Table S5. The labelings are based on the conclusion above that the intrinsic isotope shift is too small to be resolved. Also listed are the intensities calculated according to the following logic: We seek $p(r,r')$ ($r = 0,1,2 = r'$), the joint probability that the carboxyl adjacent to an ipso carbon bears $r = 0, 1, \text{ or } 2$ ¹⁸O's and that the other carboxyl bears $r' = 0, 1, \text{ or } 2$ ¹⁸O's. These probabilities too can be estimated from the mass-spectrometric $P(n)$ in Table 1, which can be separated into the contribution to each of the ipso carbon types of Figure 3. Carbons **B_{01/12}** and **B_{10/21}** each represent half of the monolabeled probability, $P(1)$, plus half of the trilabeled probability, $P(3)$. Carbons **B_{00/11}** represent the sum of the unlabeled probability, $P(0)$, the tetralabeled probability, $P(4)$, which is negligible, and two thirds of the dilabeled probability, $P(2)$. The two thirds is again because a second ¹⁸O is twice as likely to be on the other carboxyl as it is to be on an already labeled one. The remaining one third of $P(2)$ is divided in two to represent **B₀₂** and **B₂₀**. The results of this analysis are listed in Table S5. The values compare favorably with the relative peak heights h from Figure 4, with a root-mean-square deviation of 0.016. The assignment is further supported by the

addition of authentic unlabeled monoanion, which increased the center signal.

Table S5. Relative peak heights h of each ipso carbon in Figure 4 and the distribution $p(r,r')$

calculated from $P(n)$ in Table 1.			
Signal	h	Corresp	$p(r,r')$
B₀₂	0.070	$1/6P(2)$	0.061
B_{01/12}	0.251	$1/2P(1)+1/2P(3)$	0.269
B_{00/11}	0.365	$P(0)+2/3P(2)+P(4)$	0.339
B_{10/21}	0.252	$1/2P(1)+1/2P(3)$	0.269
B₂₀	0.062	$1/6P(2)$	0.061

Although Figure 4 assigns **B_{10/21}** as more shielded than **B_{01/12}** and **B₀₂** as more shielded than **B₀₂**, it must be admitted that the labels could be reversed. However, the following analysis supports the labeling made here: In CDCl₃ the ¹³C NMR signal from the ipso carbon in unlabeled diacid **2** is 135.7 ppm, more shielded than the 139.1 ppm from unlabeled monoanion **5**. Thus we may conclude that carboxylic-acid character is more shielding than carboxylate character, as was observed previously at both carboxyl and ipso carbons.⁶ Moreover, it is well established that an ¹⁶O acid is ~1% stronger than an ¹⁸O acid.⁷ Then in a double-well potential the proton resides more often on a more basic ¹⁸O-containing carboxyl than on a less basic ¹⁶O-containing carboxyl. An ¹⁸O-containing carboxyl then has more carboxylic-acid character and is shielded, relative to the ¹⁶O carboxyl, which has more carboxylate character and is deshielded. This is the basis for the assignments in Figure 4. Nevertheless, even if this assignment is reversed, the final conclusion is not invalidated.

Temperature Dependence of Ipso Shifts. Figure 5 shows how the chemical shift for each ipso carbon of ¹⁸O-labeled **5** changes as the temperature decreases. Table S6 lists the chemical shifts at these temperatures.

Table S6. ^{13}C NMR chemical shifts (ppm) for ipso carbons of ^{18}O isotopologues of **5** at various temperatures (K) in CDCl_3 .

Peak	293.9	264.1	254.1	244.2	224.3
B₀₂	139.3765	139.4331	139.4589	139.4872	139.5373
B_{01/12}	139.3524	139.4082	139.4330	139.4595	139.5061
B_{00/11}	139.3292	139.3828	139.4067	139.4327	139.4794
B_{10/21}	139.3064	139.3570	139.3808	139.4060	139.4507
B₂₀	139.2832	139.3318	139.3555	139.3800	139.4217

Conversion of slopes in Figure 5 to thermodynamic parameters. Equation 4 relates the temperature dependence of the isotope shifts to the Gibbs-energy difference (actually $\Delta\Delta G^\circ$, or $-RT\ln(K_a^{16}/K_a^{18})$). The necessary parameter D , as defined in Equation 3, can be approximated as -6.8 ppm, twice the chemical-shift difference between the ipso signals in the unlabeled diacid (135.7 ppm) and monoanion (139.1 ppm) in CDCl_3 .

References

1. Bailey, M. E.; Amstutz, E. D. *J. Am. Chem. Soc.* **1956**, *78*, 3828-3830.
2. Via http://cavanagh-lab.bch.ncsu.edu/new/intranet/temp_calb.html (accessed Sept. 27, 2013).
3. Perrin, C. L.; Thoburn, J. D. *J. Am. Chem. Soc.* **1992**, *114*, 8559-8565.
4. Silverstein, R. M.; Bassler, G. C.; Morrill, T. C. *Spectrometric Identification of Organic Compounds*; John Wiley & Sons: New York; 5th ed., **1991**, pp 117-118.
5. Perrin, C. L.; Thoburn, J. D. *J. Am. Chem. Soc.* **1989**, *111*, 8010-8012.
6. Perrin, C. L.; Nielson, J. B. *J. Am. Chem. Soc.* **1997**, *119*, 12734-12741.
7. Ellison, S. L. R.; Robinson, M. J. T. *J. Chem. Soc. Chem. Commun.* **1963**, 745-746. Knight, W. B.; Weiss, P. M.; Cleland, W. W. *J. Am. Chem. Soc.* **1986**, *108*, 2759-2761. Perrin, C. L. *Adv. Phys. Org. Chem.* **2010**, *44*, 123-171.